AD-A046 923 ARIZONA UNIV TUCSON DEPT OF AEROSPACE AND MECHANICA--ETC F/G 20/4
SMALL UNSTEADY PERTURBATIONS IN TRANSONIC FLOWS,(U)
NOV 77 K FUNG , N J YU, R SEEBASS N00014-76-C-0182

UNCLASSIFIED NL

1 OF 1
ADA046923

END
DATE FILMED
12-77
DDC

AD A046923

UNCLASSIFIED

SECURITY CLASSIFICATION OF THIS PAGE (When Data Entered)

12 B.S.

REPORT DOCUMENTATION PAGE	READ INSTRUCTIONS BEFORE COMPLETING FORM
1. REPORT NUMBER	2. GOVT ACCESSION NO. 3. RECIPIENT'S CATALOG NUMBER
4. TITLE (and Subtitle) SMALL UNSTEADY PERTURBATIONS IN TRANSONIC FLOWS, (6)	5. TYPE OF REPORT & PERIOD COVERED 6. PERFORMING ORG. REPORT NUMBER
7. AUTHOR(s) (10) K-Y. Fung, N. J. Yu[redacted] R. Seebass	8. CONTRACT OR GRANT NUMBER(s) N00014-76-C-0182, (15) AFOSR-76-2954
9. PERFORMING ORGANIZATION NAME AND ADDRESS University of Arizona, Aerospace and Mechanical Engineering, Tucson, Arizona 85721	10. PROGRAM ELEMENT, PROJECT, TASK AREA & WORK UNIT NUMBERS NR 061-231
11. CONTROLLING OFFICE NAME AND ADDRESS Office of Naval Research (code 438) Arlington, Virginia 22217 (12) 30 p.	12. REPORT DATE (11) Nov[redacted]77 13. NUMBER OF PAGES 29
14. MONITORING AGENCY NAME & ADDRESS (if different from Controlling Office) ONR Resident Representative, Room 421-Space Science Building, University of Arizona, Tucson, Arizona 85721	15. SECURITY CLASS. (of this report) Unclassified 15a. DECLASSIFICATION/DOWNGRADING SCHEDULE
16. DISTRIBUTION STATEMENT (of this Report) Approved for Public Release; distribution unlimited.	DDC RECEIVED NOV 16 1977 B
17. DISTRIBUTION STATEMENT (of the abstract entered in Block 20, if different from Report)	
18. SUPPLEMENTARY NOTES	
19. KEY WORDS (Continue on reverse side if necessary and identify by block number) Transonic flow, Unsteady flow	
20. ABSTRACT (Continue on reverse side if necessary and identify by block number) The effects of very small, low frequency, perturbations to steady transonic flows are investigated for two-dimensional flows described by the small perturbation equation. A method that allows one to account for shock wave motions due to arbitrary, but small, unsteady changes in the boundary conditions is described. Both harmonic and indicial responses may be calculated. Time-linearized results for transonic flow past an NACA 64A006 airfoil experiencing harmonic motions in one of several modes are presented.	

DD FORM 1 JAN 73 1473 EDITION OF 1 NOV 65 IS OBSOLETE S/N 0102-LF-014-6601

UNCLASSIFIED 402 192

SECURITY CLASSIFICATION OF THIS PAGE (When Data Entered)

AU No. DDC FILE COPY

SMALL UNSTEADY PERTURBATIONS IN TRANSONIC FLOWS[†]

K-Y. Fung[*], N. J. Yu[**] and R. Seebass[***]
University of Arizona
Tucson, Arizona 85721

Abstract

We investigate the effects of very small, low frequency, perturbations to steady transonic flows. We do so in the context of two-dimensional flows described by the small perturbation equation. We draw inferences from an even simpler model equation. Our primary concern is with the validity of linearizing the unsteady perturbations to such flows and, in particular, with the failure of earlier studies to account for the shock wave motions that we know occur. We provide a method that allows one to account for shock wave motions due to arbitrary, but small, unsteady changes in the boundary conditions. Consequently, both harmonic and indicial responses may be determined. Time-linearized results for the transonic flow past an NACA 64A006 airfoil experiencing harmonic motions in one of several modes are presented. Selected results are compared with those obtained from nonlinear calculations using a shock-fitting algorithm.

† This research was sponsored by the AFOSR through Grant 76-2954 and the ONR through Grant N0014-76-C-0182.

* Senior Research Associate, Member AIAA.
** Senior Research Associate, Member AIAA.
*** Professor, Associate Fellow AIAA.

Introduction

In unsteady transonic flows, relatively small periodic changes in the boundary conditions can lead to substantial changes in the magnitude and phase lag of loads and moments. These are of major concern in the aerodynamic design of aircraft that operate in the transonic regime. Reference 1 contains a short, but timely, review of various aspects of unsteady transonic flow. Of particular concern are aeroelastic behavior and flutter boundaries. Here the unsteady perturbations may be considered small, and linearization about a nonlinear steady flow, as suggested by Landahl[2] long ago, would seem to be appropriate. Difficulties arise, however, that detract from this procedure. While the equation is linear, its coefficients are variable and must be determined by numerical solution of a nonlinear problem that, in the cases of prime interest, has a discontinuous solution; that is, there are embedded shock waves. Also, while a change of variables in the linear equation provides a scaling of parameters that is indicative of the trade-offs between, e.g., Mach number and reduced frequency, the only similitude is the one basic to the nonlinear formulation.

Traci et al.[3,4] have developed relaxation methods for solving the resulting time-linearized equations of motion. Less complete, but comparable, studies have been made by Weatherill et al.[5]; these derive from an earlier study by Ehlers[6]. In both of these studies shock motions, which contribute substantially to the time varying loads and moments,[7,8] are neglected. Also, difficulties arise in the convergence of the iterative numerical scheme.

Here we pursue a different numerical course. Yu et al.[9] have developed a numerical procedure for computing solutions to the unsteady small perturbation equation for transonic flows, which treats embedded shock waves as discontinuities. This procedure can be used to calculate the basic steady flow

that we wish to subject to small unsteady perturbations. A simplified version of this algorithm can then be used to calculate the linearized unsteady perturbations to the flow. These calculations can be carried out in conjunction with an algorithm that determines the shock wave motion. The procedure we have used to calculate the shock wave motion is a rather obvious one; it is not surprising then, that it, too, was given in the monograph by Landahl[2] (Section 10.2). An alternative procedure, related in some ways to that used here, is implied by Nixon's[10] study of perturbations to steady discontinuous transonic flows.

After a brief review of the formulation of time-linearized methods, we discuss a one-dimensional model equation. This provides a suitable testing ground for our ideas and serves to illustrate several basic points we wish to stress. Next, we discuss the two-dimensional formulation and compare results of time-linearized calculations with those obtained without the linearization, for an NACA 64A006 airfoil oscillating in pitch.

Formulation

We write the unsteady small disturbance equation for low frequency transonic flows in the commonly used form

$$-2KM_\infty^2\phi_{xt} + \{1 - M_\infty^2 - (\gamma + 1)M_\infty^2\phi_x\}\phi_{xx} + \phi_{yy} = 0. \qquad (1)$$

The spatial coordinates, the time, and the velocity potential in (1) have been non-dimensionalized by the chord, the reciprocal of the angular frequency, and the free stream velocity times the chord, respectively. Other, perhaps more suitable, forms are given in Reference 9. This equation results from a

systematic expansion of the velocity potential in the thickness ratio τ and applies for reduced frequencies $K = 0(\tau^{2/3})$, where $K = \omega c/U$, i.e., the angular frequency multiplied by the time it takes the flow to traverse the airfoil chord. Lin, Reisner and Tsien[11] showed that, with restriction to small perturbations throughout the flow, (1) is the only nonlinear equation that arises. For moderate frequencies the equation

$$-K^2\phi_{tt} - 2K\phi_{xt} + \{1 - M_\infty^2 - (\gamma + 1)M_\infty^2[\phi_x + \frac{\gamma - 1}{\gamma + 1} K\phi_t]\}\phi_{xx} + \phi_{yy} = 0$$

is frequently used, with or without the ϕ_t term, and may provide results that apply at higher frequencies than those obtained from (1) or the linear form of the above equation.[3]

Because $K = 0(\tau^{2/3})$, the boundary condition on the body takes the simple form

$$\phi_y(x,0,t) = \tau\partial Y(x,t)/\partial x = \tau[Y^\circ_x + \frac{\delta}{\tau}(Y^u_x + KY^u_t)], \quad -\frac{1}{2} \le x \le \frac{1}{2} \tag{2}$$

where $Y(x,t)$, the instantaneous body shape, has been decomposed into a steady part, Y°, and an unsteady part, Y^u. The last term, KY^u_t, is dropped except when Y^u_x is small or zero because $K = 0(\tau^{2/3})$. Here δ is the amplitude of the unsteady oscillation. Far from the body we require that the derivatives of ϕ vanish. In this approximation the pressure coefficient, defined so that it vanishes at sonic conditions, takes the form

$$C_p = -2\left\{\frac{M_\infty^2 - 1}{(\gamma + 1)M_\infty^2} + \phi_x\right\}. \tag{3}$$

In the small disturbance approximation, the Kutta condition is imposed by requiring that C_p be continuous at $y = 0$ for $x > 1/2$.

Any shock wave that exists in the flow field must satisfy the jump relation derived from the conservative form of the governing equation (1), namely,

$$-2KM_\infty^2[\![\phi_x]\!]^2\left(\frac{dx}{dt}\right)_s - \{1 - M_\infty^2 - (\gamma+1)M_\infty^2\tilde{\phi}_x\}[\![\phi_x]\!]^2 + [\![\phi_y]\!]^2 = 0 \tag{4}$$

together with the condition derived from the assumption of irrotationality,

$$\left(\frac{dy}{dx}\right)_s = -[\![\phi_x]\!]/[\![\phi_y]\!]. \tag{5}$$

Here $\tilde{\phi}_x$ refers to the mean value of ϕ_x evaluated on each side of the discontinuity, and $[\![\phi_x]\!]$ indicates the jump in ϕ_x across the discontinuity; the subscript "s" denotes the quantity evaluated at the shock surface.

Time-Linearized Equations

We now assume that the unsteady disturbances, characterized by δ, are small enough that we may write

$$\phi(x,y,t) = \phi^\circ(x,y) + \delta\psi(x,y,t) + o(\delta) \tag{6}$$

and neglect higher-order terms in δ. The restriction imposed on δ for this to be true will depend on the other parameters of the problem, viz., $\kappa \equiv (1 - M_\infty^2)/[(\gamma+1)M_\infty^2\tau]^{2/3}$ and K. This gives

$$\{1 - M_\infty^2 - (\gamma+1)M_\infty^2\phi_x^\circ\}\phi_{xx}^\circ + \phi_{yy}^\circ = 0$$

$$\phi_y^\circ(x,0) = \tau Y^{\circ\prime}(x), \quad -\frac{1}{2} \le x \le \frac{1}{2} \tag{7}$$

and

$$-2KM_\infty^2\psi_{xt} + \{[1 - M_\infty^2 - (\gamma + 1)M_\infty^2\phi_x^\circ]\psi_x\}_x + \psi_{yy} = 0$$

$$\psi_y(x,0,t) = Y_x^u(x,t), \qquad -\frac{1}{2} \le x \le \frac{1}{2}. \tag{8}$$

The solution to (7) must satisfy the steady version of the shock relations (4) and (5). The shock relations for (8) are discussed later.

As mentioned above, a shock-fitting scheme that approximates the shock waves as discontinuities normal to the free stream has been developed[9] with an alternating-direction implicit scheme (i.e., ADI) to compute the solution to (7). Comparison of these results with the results obtained[12] using an exact shock-fitting algorithm and line relaxation indicate that they should suffice for most studies. At the very least they should prove adequate for the time-linearized studies of interest here, as only small shock excursions can be allowed.

We assume, then, that we have the numerical values for ϕ_x° required in (8). These data will be discontinuous across some vertical line, the shock wave, $x = x^*$, $0 \le |y| \le y^*$. We then ask, under what conditions is (8) valid? And how do we account for shock wave motions in the linearized analysis? The answers to these questions are inferred from a simple one-dimensional model discussed in the next section.

Anticipating that we will wish to solve (8) with the same technique that proved successful for (1) we avoid writing

$$\psi(x,y,t) = \mathrm{Re}\{\bar{\psi}(x,y)e^{i\omega t}\}. \tag{9}$$

The assumption (9) restricts the study to harmonic linear motions. Because indicial motions can be superimposed to obtain the results for any frequency,

they too seem important. The assumption (9) suppresses the time dimension of the calculation but it results in two coupled equations, or one equation for a complex-valued $\bar{\psi}$, which may be solved by line relaxation. Our experience with unsteady ADI techniques has been that they are at least as effective as line relaxation for problems of this type, and hence there is no numerical advantage to the decomposition (9). This conclusion was also arrived at by Ballhaus et al.[13] in a related study.

An appropriate scaling of the dependent and independent variables in (7) and (8) allows either the thickness or the frequency to be normalized to the value 1, as expected. This scaling, in terms of the transonic similarity parameter κ, the amplitude of the unsteady motion δ, its frequency ω, and the body's basic thickness τ, leads to

$$\psi(\tilde{x},\tilde{y};\kappa;\delta;\omega;1) = \omega\tilde{\psi}\left(\tilde{x},\frac{\tilde{y}}{\omega^{1/2}};\frac{\kappa}{\omega^{1/2}};1;\frac{1}{\omega^{1/2}}\right)$$

where $\tilde{x}$ and $\tilde{y}$ are suitably scaled replacements for the x and y coordinates. This result can be used to check trends noted in the numerical results.

One-Dimensional Model

To answer the questions raised above, we study a simple unsteady one-dimensional analog of (2). We consider a one-dimensional unsteady equation that models the important features of (2), and ascertain how a simple steady solution is modified by small unsteady perturbations. We consider, then,

$$2\phi_{xt} + (1 - \phi_x)\phi_{xx} = 2\phi_{xt} - \frac{1}{2}\{(1 - \phi_x)^2\}_x = 0 \qquad (10)$$

subject to $\phi(0,t) = f_1(t)$, $\phi_x(0,t) = f_2(t)$ and either $\phi(1,t)$ or $\phi_x(1,t) = f(t)$. There are restrictions on f which, for brevity, we do not list. Our

study could be generalized by replacing $1 - \phi_x$ in (10) by $(A(x) - \phi_x)$ where $A(x)$ is a continuous function of x, but little added insight is gained.

To simplify matters further, consider the especially simple subcase $f_1 = 0$, $f_2 = -1$, $f = 3 + \delta p(t)$. When $\delta \equiv 0$, we have the steady solution

$$\phi^\circ = \begin{cases} -x, & 0 \le x \le 3/4 \\ -3(1 - x), & 3/4 \le x \le 1. \end{cases}$$

This satisfies (10) and the jump condition that one derives from it, viz.,

$$[\![\phi]\!] = 0 \quad \text{on} \quad 2\frac{dx_s}{dt} = 1 - \tilde{\phi}_x. \tag{11}$$

Now a general solution of (10), in terms of ϕ_x, is

$$\phi_x = \text{arbitrary function of } \left(t + \frac{2(1 - x)}{1 - \phi_x} \right).$$

This can be verified by substitution. With, say $\phi_x(1,t) = 3 + \delta p(t)$ we have, for $x > x_s$,

$$\phi(x,t) = 3(x - x_s) + \delta \int_{x_s}^{x} p\left(t + \frac{2(1 - \hat{x})}{1 - \phi_x(\hat{x},t)} \right) d\hat{x} - h(t) \tag{12}$$

where the choice $h(t) = x_s(t)$ insures that $[\![\phi]\!] = 0$ at $x = x_s$ because $\phi = \phi^\circ$ for $x < x_s$.

The shock motion must be determined by the direct integration of (11):

$$2\frac{dx_s}{dt} = 1 - \tilde{\phi}_x = -\frac{\delta}{2} p(x_s(t),t). \tag{13}$$

Now, for comparison, we determine the results that are obtained by time linearization; i.e., we write

$$\phi(x,t;\delta) = \phi^\circ(x) + \delta\psi(x,t) + o(\delta) \tag{14}$$

and solve the linear equation for ψ that results by dropping higher-order terms in δ. That is, we solve

$$2\psi_{xt} + (1 - \phi^\circ_x)\psi_{xx} - \phi^\circ_{xx}\psi_x = 0 \tag{15}$$

subject to $\psi_x(1,t) = p(t)$.

We now linearize the first of equations (11) as follows:

$$[\![\phi(x,t)]\!] = 0 = [\![\phi(x^\circ_s,t) + \phi_x(x^\circ_s,t)(x_s(t) - x^\circ_s) + \ldots]\!]$$

$$= [\![\phi^\circ(x^\circ_s) + \delta\psi(x^\circ_s,t) + \phi^\circ_x(x_s(t) - x^\circ_s)]\!].$$

Thus we conclude that

$$\delta\,[\![\psi(x^\circ_s,t)]\!] = -[\![\phi^\circ_x(x^\circ_s)]\!](x_s - x^\circ_s). \tag{16}$$

From the second equation of (11), with $x_s(t) = x^\circ_s + \delta\chi(t)$ we find

$$\frac{d\chi}{dt} = -\frac{1}{2}\tilde{\psi}_x = -\frac{1}{4}\psi_{x_b}$$

where $(\,)_b$ refers to the value behind the shock. Thus we may replace (11) by

$$[\![\psi(x_s^\circ,t)]\!] = -[\![\phi_x^\circ(x_s^\circ)]\!]\chi$$

or

$$\psi_b(x_s^\circ,t) = -4\chi(t), \tag{17a}$$

and

$$\frac{d\chi}{dt} = -\frac{1}{4}\psi_{x_b}. \tag{17b}$$

Example

Consider now, for example,

$$p(t) = \sin \omega t;$$

it is easy to show that a general solution to (15) is

$$\psi(x,t) = -\frac{1}{\omega}[\cos \omega(1 - x - t) - h(t)].$$

The function $h(t)$ follows from (17a,b) and assuming, e.g., that $\psi(3/4,0) = 0$. Thus

$$\psi(x,t) = -\frac{1}{\omega}[\cos \omega(1 - x - t) - \cos(\omega/4)] \tag{18}$$

and

$$\chi(t) = \frac{1}{4\omega}[\cos \omega(\tfrac{1}{4} - t) - \cos(\omega/4)]. \tag{19}$$

Had we solved (15) with $\psi \equiv 0$ for $x < x_s(t)$ and determined the exact shock motion from (11) with $1 - \phi_x = -2 + O(\delta)$ used in (12), we would find that behind the shock

$$\phi(x,t) = \phi^\circ + 3 - 4x_s - \frac{\delta}{\omega}[\cos \omega(1 - x - t) - \cos \omega(1 - x_s - t)], \tag{20}$$

where the shock motion is given explicitly by

$$x_s = \frac{2}{\omega} \tan^{-1} \left\{ \frac{\tan \frac{\omega}{2} (t + c) - [\tan \frac{\omega}{2} (t - 1) - \frac{\delta}{4}]}{1 + \tan \frac{\omega}{2} (t - 1)[\tan \frac{\omega}{2} (c + t) + \frac{\delta}{4}]} \right\}, \tag{21}$$

with $c = -2(\tan^{-1} [\tan (\omega/8) + \delta/4])/\omega$. For $\omega >> \delta$, which is required for small shock motions, (21) simplifies to

$$x_s = \frac{3}{4} + \frac{\delta}{4\omega} [\cos \omega(\frac{1}{4} - t) - \cos (\omega/4)].$$

Thus these results are in agreement with (18) and (19) to lowest order in δ.

The time-linearized results (18) and (19) are now compared with the exact results. The nonlinear result for $x > x_s$, given by (12) and (13), is

$$\phi = \phi^\circ + 3 - 4x_s(t) + \delta \int_{x_s}^{x} \sin \omega \left(t + \frac{2(1 - \hat{x})}{1 - \phi_x(\hat{x},t)} \right) d\hat{x} \tag{22}$$

where

$$\frac{dx_s}{dt} \equiv \dot{x}_s = -\frac{\delta}{4} \sin \omega \left(t + \frac{1 - x_s}{1 - 2\dot{x}_s} \right). \tag{23}$$

The results (22) and (23) are consistent with the time-linearized results (18) and (19) to $0(\delta)$, except for a slow secular drift in the shock position of $0(\delta^2 t)$ that occurs in (23) but not in (19). This is an artifact of our one-dimensional model; even if it were not, it would not invalidate the use of the linear results for flutter studies where δ is small and structural damping determines the time scale of interest.

The time-linearized result for ϕ, given by (14) and (18), is shown in Figure 1 for $\delta = 0.1$ with $\omega = 0.5$. The shock motion (19) is shown in Figure 2,

again for $\delta = 0.1$ and with $\omega = 0.5$, 1.0 and 2.0. As is clear from (19), the shock excursions are $O(\delta/\omega)$. Consequently, they cannot be neglected in the calculation unless δ/ω is much smaller than one. For the times shown, there is no significant difference between the results (19) and (23) due to the $O(\delta^2 t)$ term.

The main conclusions we derive from this study are that it is essential to consider shock motion in computing time-linearized solutions if we are to determine the effects of small unsteady perturbations correctly to lowest order, and that shock excursions increase as the frequency is decreased. Additionally, this motion can be computed in a straightforward manner.

Two-Dimensional Time-Linearized Analysis

The results from our simple model show that the time-linearized results must be corrected for shock motions if they are to be consistently correct to lowest order. This can be accomplished by calculating the shock motion in conjunction with the time-linearized solution. Here we follow an analogous procedure and calculate the change with time of the values of the perturbed potential behind the shock required by the linearized shock jump relations. Thus, we wish to solve (8)

$$-2KM_\infty^2\psi_{xt} + \{[1 - M_\infty^2 - (\gamma + 1)M_\infty^2\phi_x^\circ]\psi_x\}_x + \psi_{yy} = 0$$

with (8)

$$\psi_y(x,0,t) = Y_x^u(x,t), \quad -\frac{1}{2} \leq x \leq \frac{1}{2}$$

subject to the far-field boundary and Kutta conditions. As we noted, the steady result for ϕ_x° can be calculated adequately for most small disturbance flows using normal shock fitting as described in Reference 9. Under the assumption that the shock wave is normal, the shock jump conditions (4) and

(5) can be replaced by requiring

$$[\![\phi]\!] = 0 \quad \text{on} \quad \frac{dx_s}{dt} = \frac{\gamma + 1}{2K} \left\{ \frac{M_\infty^2 - 1}{(\gamma + 1)M_\infty^2} + \tilde{\phi}_x \right\} . \tag{24}$$

For steady flow $\dot{x}_s = 0$ and in (24) $\{\cdots\} = 0$. We express the shock position as

$$x_s = x_s^\circ + \delta\chi(t)$$

and conclude that the shock motion is governed by

$$\frac{d\chi}{dt} = \frac{\gamma + 1}{2K} \tilde{\psi}_x .$$

As discussed in Reference 9, $\tilde{\psi}_x$ is evaluated at $y = 0$. On the shock

$$[\![\phi]\!] = [\![\phi^\circ]\!] + \delta[\![\psi]\!]; \tag{25}$$

linearizing the expression (25) for the velocity potential about the steady shock position we find

$$\phi(x_s,y,t) = \phi(x_s^\circ,y,t) + \phi_x(x_s^\circ,y,t)\delta d\chi$$

$$= \phi^\circ(x_s^\circ,y) + \phi_x^\circ(x_s^\circ,y)\delta d\chi + \delta\psi(x_s^\circ,y,t) + O(\delta^2).$$

Because we have treated the shock as a normal one, y appears here simply as a parameter. Now $[\![\phi(x_s,t,y)]\!]$ and $[\![\phi^\circ(x_s^\circ,y)]\!]$ are both zero; consequently we have

$$[\![\psi(x_s^\circ,y,t)]\!] = -\frac{(\gamma+1)}{2K}[\![\phi_x^\circ(x_s^\circ,y)]\!]\int_0^{\tilde{t}}\psi_x(x_s^\circ,0,\hat{t})d\hat{t} \tag{26}$$

which must be integrated in time in conjunction with the solution to (8).

Equation (8) is now solved numerically in time and space in conjunction with (26), which is used to update the values of ψ behind the shock. We start with a steady solution and initiate a body motion, such as the harmonic oscillation of a flap. The calculations proceed in time until they are judged to be periodic. Note that indicial as well as harmonic motions may be considered because we have not utilized the usual harmonic decomposition (9).

Numerical Procedure

The numerical procedure used here derives from that developed for the nonlinear equation (1). The main simplification occurs in the shock jump conditions. In order to minimize the far-field boundary effects on the results which, as Magnus[14] has noted, can be significant, we again use coordinate stretching[9] in the form:

$$\xi = \pm[1 - \exp(-a_1|x|)] \quad \text{for} \quad x \gtrless 0,$$

$$\eta = \pm[1 - \exp(-a_2|y|)] \quad \text{for} \quad y \gtrless 0,$$

where a_1 and a_2 are constants that determine the mesh distribution. This stretching transforms the infinite physical domain into a computational domain bounded by $|\xi| \leq 1$ and $|\eta| \leq 1$. The mesh distribution is concentrated on the airfoil. In these coordinates (8) becomes

$$A_1\{\psi_\xi\}_t + A_2\{f(\xi,\eta)(1-|\xi|)\psi_\xi\}_\xi + A_3\{(1-|\eta|)\psi_\eta\}_\eta = 0 \tag{27}$$

where

$$A_1 = \frac{-2KM_\infty^2 a_1}{a_2(1 - |\eta|)}, \quad A_2 = \frac{a_1^2}{a_2(1 - |\eta|)}, \quad A_3 = \frac{a_2}{1 - |\xi|}$$

and

$$f(\xi,\eta) = 1 - M_\infty^2 - a_1(\gamma + 1)M_\infty^2(1 - |\xi|)\phi_\xi^\circ$$

is known in discrete form from the steady numerical solution. This function is discontinuous at $\xi = \xi_s^\circ$ for $0 \le \eta \le \eta^*$. First-order backward time and spatial differences are used for the first term. Centered or first-order backward differences are used for the second term if f is less than or greater than zero, respectively; $f(\xi,\eta)$ is known in advance with the derivative ϕ_ξ° automatically evaluated correctly. Centered differences are used for the third term and denoted by δ_η.

The solution is computed using an alternating-direction implicit procedure first applied to transonic flow problems by Ballhaus and Steger[15] and by Beam and Warming[16], and subsequently further refined by Ballhaus and Goorjian[17]. The solution is advanced in time from its initial steady state to subsequent time levels with the following two-step procedure.

New values of ψ, denoted by ψ^+, are calculated along η = constant lines using

$$A_1 \frac{\psi_\xi^+ - \psi_\xi^n}{\Delta t} + A_2\{f(\xi,\eta)(1 - |\xi|)\psi_\xi^+\}_\xi + A_3\delta_\eta\{(1 - |\eta|)\psi_\eta^n\} = 0.$$

This is coupled with the computation of new values of ψ^+ behind the shock obtained by using (26). With the shock located at ξ_s° such that $\xi_s < \xi_s^\circ < \xi_{s+1}$, we can express the values of ψ ahead of and behind the

shock in a Taylor series, finally arriving at the result

$$[\![\psi]\!]^{+} = -C(\eta)\Delta t\tilde{\psi}_{\xi}^{n} + [\![\psi]\!]^{n} \tag{28}$$

where

$$C(\eta) = \frac{\gamma + 1}{4K} a_1^2(1 - |\xi_s^\circ|)^2[\![\phi_\xi^\circ(\xi_s^\circ,\eta)]\!]$$

and $\tilde{\psi}_{\xi}^{n}$ is evaluated, following (26), at $\eta = 0$. One-half the change in ψ across the shock is accounted for in this step, effectively using the trapezoidal rule in the time integration (26); hence C is half the value implied by (26).

With the values of ψ^{+} determined, the new values of ψ at the subsequent time level, ψ^{n+1}, are calculated using

$$A_1 \frac{\psi_\xi^{n+1} - \psi_\xi^{+}}{\Delta t} + \frac{A_3}{2}\delta_\eta\{(1 - |\eta|)(\psi_\eta^{n+1} - \psi_\eta^{n})\} = 0$$

in conjunction with the completion of the time integration (26),

$$[\![\psi]\!]^{n+1} = -C(\eta)\Delta t\tilde{\psi}_{\xi}^{n+1} + [\![\psi]\!]^{+}. \tag{29}$$

Again, $\tilde{\psi}_{\xi}^{n+1}$ is evaluated at $\eta = 0$.*

The full procedure is, effectively,

$$A_1 \frac{\psi_\xi^{n+1} - \psi_\xi^{n}}{\Delta t} + A_2\{f(\xi,\eta)(1 - |\xi|)\psi_\xi^{+}\}_\xi + \frac{1}{2}A_3\delta_\eta\{(1 - |\eta|)(\psi_\eta^{n+1} + \psi_\eta^{n})\} = 0$$

---

*The results given by the authors in AIAA Paper No. 77-675 were in error because $\tilde{\psi}_\xi$ was allowed to vary with η; this is not consistent with the normal shock approximation that gives (24).

with (26) implemented in the form (28), (29). The procedure outlined here effectively corrects the ψ values for shock motions as the solution progresses. The shock motion is easily determined simultaneously by using (26) and the expression for $d\chi/dt$ to find

$$\chi^{n+1}(0,t) = -[\![\psi(x_s^\circ,0,t)]\!]^{n+1}/[\![\phi_x(x_s^\circ,0)]\!]. \tag{30}$$

The computations then provide results for ϕ_x like those sketched in Figure 3. This figure depicts the steady state result and the unsteady changes as well as the shock positions at two different time levels where the shock is behind the steady state position. When the shocks have been inserted in their known positions we see that we need to analytically continue data ahead of and behind the shock in order to complete the solution. For shock excursions that are o(1) we can simply extrapolate the steady state data, both ahead of and behind the shock, to determine the pressure distribution on the body correctly to lowest order. Larger shock motions are, of course, not admissable in this theory.

Results and Discussion

Time-linearized results have been computed for an NACA 64A006 airfoil experiencing harmonic pitching and flap motions. As noted earlier, in the low frequency approximation made here, pitching and plunging motions lead to the same result except that the time-linearized perturbations are proportional to the maximum pitch angle for the former, and K times the maximum amplitude for the latter. Harmonic motions initiated from a steady state become nearly periodic in three to ten cycles, with the changes induced by flap oscillations

becoming periodic more rapidly than those resulting from pitching oscillations. More cycles were required for larger reduced frequencies and, to a lesser degree, higher Mach numbers.

In order to confirm the validity of the time-linearized calculations, both the time-linearized and nonlinear algorithms were used to compute the response to a step change in angle of attack and the harmonic response to pitching motions. Figure 4 compares the nonlinear and time-linearized results for the normalized circulation and shock position for harmonic pitching motions at $M_\infty = 0.88$ and $K = 0.48$. For these conditions very small unsteady changes lead to very small shock motions and in both calculations the shock wave remains between grid points. Because of the extrapolation procedure used in the nonlinear shock-fitting, the finite mesh size used can introduce errors, albeit small ones, in the shock's position when a grid line is crossed. We wished to eliminate these errors in order to use the nonlinear calculations to judge the accuracy of time-linearized calculations. These results indicate that for pitching about mid-chord, nonlinear, amplitude dependent, behavior occurs for $\delta/\tau \geq 0.1$ for $K = 0.48$. Because the amplitude of the shock motion increases with decreasing K, nonlinear effects occur at smaller values of δ/τ at lower reduced frequencies. Results are given for the fifth cycle; note that the nonlinear results are not yet periodic. Figure 5 compares the nonlinear and time-linearized pressure deviation from steady state at six angular times for the same conditions. Good agreement between the results is obtained for δ/τ less than 0.1.

Time-linearized pressure distributions at six angular positions for an oscillating quarter-chord flap with $K = 0.06$ and $M_\infty = 0.875$ are shown in Figure 6. The flap deflection is downward during the first half of the cycle. The results for the second half of the period, for the symmetrical problem

shown here, are just the results shown with the lower and upper surface pressures interchanged. Thus the results for $0°$ are not given as they are just those for $180°$ with the lower and upper surface pressures reversed. Because the flap hinge occurs very close to the steady state shock location, the pressure singularity due to the change in flow direction at the hinge is missed. The circulation and shock excursion obey the following relations:

$$\Gamma(t)/\delta = 9.26 \sin (t - 59°),$$

$$\chi(t) = 12 \sin (t - 51°).$$

Note the substantial phase lag in the circulation and the shock's position.

Time-linearized pressure distributions at six angular positions for an oscillating airfoil with $K = 0.12$ and $M_\infty = 0.875$ are depicted in Figure 7. If these results are multiplied by K, then they represent the pressure perturbations for a plunging airfoil. As in the previous case of an oscillating flap, changes in forces and moments of $0(\delta/K)$ occur due to shock wave motion. In this case

$$\Gamma(t)/\delta = 5.48 \sin (t - 70°),$$

$$\chi(t) = 5.62 \sin (t - 87°).$$

Analogous computations have been carried out for $K = 0.06$, 0.12, 0.24 and 0.48. Figure 8 depicts the shock wave's excursion and maximum circulation as a function of K^{-1}. The nearly linear variation of the shock excursion substantiates an observation made in a one-dimensional model where the shock wave excursion is directly proportional to $1/K$.

In these calculations the circulation gives an immediate evaluation of the lift coefficient as a function of time; the moment coefficient must be evaluated by integrating the moment of the pressure coefficient. This is done by integrating the moment of pressure perturbations with the shock wave in its steady-state position and then correcting these results for the moment due to the shock wave motion, assuming that the shock's strength is defined by the steady-state pressure field. This makes an error in the shock strength of $O(\delta)$, but the effect on the moment is $O(\delta^2/K)$; because we have neglected other higher-order terms it is consistent to neglect this change in the strength of the shock wave.

For the time-linearized results to be valid we must really require $\delta/\tau K << 1$. Our numerical results indicate that for $\delta/\tau K \leq 0.2$ the unsteady perturbations are essentially linear.

The time-linearized algorithm used here is a derivative of that used for the nonlinear calculations. Consequently, computational times are not greatly reduced from those required for the nonlinear calculations. The linearity of these computations may make it possible to greatly reduce the computational effort required. Numerical experience has shown some difficulties for $\Delta t(\text{in degrees})/K \geq 50$. This is in agreement with the consistency requirement for the ADI algorithm used here. Both the domain of dependence condition and a local linearized stability analysis shows the procedure to be unconditionally stable. Each time step requires about two seconds of CPU time on a CDC 6400, or about 0.1 seconds on a CDC 7600. The number of time steps required for a given computation is somewhat less than those required for the nonlinear computations at small values of K, and comparable at larger values of K.

Conclusion

An accurate and efficient procedure for computing time-linearized, small perturbation, low frequency transonic flows, including shock wave motions, has been developed. Shock motions must be included as their amplitude is proportional to that of the motion divided by the reduced frequency. Both indicial and harmonic responses for various modes of motion may be computed in seconds on a CDC 7600.

References

1. Ballhaus, W. F., 1976, "Some Recent Progress in Transonic Flow Computations," VKI Lecture Series on Computational Fluid Dynamics.

2. Landahl, M. T., 1961, Unsteady Transonic Flow, Pergamon Press, New York.

3. Traci, R. M., Albano, E. D., and Farr, J. L., Jr., 1975, "Perturbation Method for Transonic Flow about Oscillating Airfoils," AIAA Paper No. 75-877.

4. Traci, R. M., Albano, E. D., Farr, J. L., Jr., and Cheng, H. K., 1974, "Small Disturbance Transonic Flows about Oscillating-Airfoils," Air Force Flight Dynamics Laboratory, Wright-Patterson Air Force Base, Ohio, AFFDL-TR-75-100.

5. Weatherill, W. A., Ehlers, F. E., and Sebastian, J. D., 1975, "Computation of the Transonic Perturbation Flow Field Around Two- and Three-Dimensional Oscillating Wings," NASA CR-2599.

6. Ehlers, F. E., 1974, "A Finite Difference Method for the Solution of the Transonic Flow About Harmonically Oscillating Wings," NASA CR-2257.

7. Tijdeman, H., 1975, "On the Motion of Shock Waves on an Airfoil with Oscillation Flap in Two-Dimensional Transonic Flow," NLR TR 75038U.

8. Tijdeman, H., 1975, "On the Motion of Shock Waves on an Airfoil with Oscillating Flap," Ed. K. Oswatitsch and D. Rues, IUTAM Symposium Transsonicum II, Göttingen, 49-56.

9. Yu, N. J., Seebass, A. R., and Ballhaus, W. F., 1977, "An Implicit Shock-Fitting Scheme for Unsteady Transonic Flows Computations," AIAA Paper No. 77-633, AIAA 3rd Computational Fluid Dynamics Conference.

10. Nixon, D., 1977, "Perturbation of Discontinuous Transonic Flow," AIAA Paper No. 77-206.

11. Lin, C. C., Reissner, E., and Tsien, H. S., 1948, "On Two-Dimensional Non-Steady Motion of a Slender Body in a Compressible Fluid," J. Math. and Physics, 27, 220-231.

12. Yu, N. J. and Seebass, R., "Accuracy of Transonic Flow Computations" (unpublished).

13. Ballhaus, W. F., Jameson, A., and Albert, J., 1977, "Implicit Approximate-Factorization of Steady Transonic Flow Problems," NASA TM X-73202.

14. Magnus, R. J., 1977, "Computational Research on Inviscid, Unsteady, Transonic Flow over Airfoils," ONR Report CASD/LVP 77-010.

15. Ballhaus, W. F. and Steger, J. L., 1975, "Implicit Approximate-Factorization Schemes for the Low-Frequency Transonic Equation," NASA TM X-73082.

16. Beam, R. M. and Warming, R. F., 1976, "An Implicit Finite-Difference Algorithm for Hyperbolic Systems in Conservation-Law Form," Journal of Computational Physics, Vol. 22, No. 1, 87-110.

17. Ballhaus, W. F. and Goorjian, P. M., 1977, "Implicit Finite Difference Computations of Unsteady Transonic Flows about Airfoils, Including the Treatment of Irregular Shock Wave Motions," AIAA Paper No. 77-205.

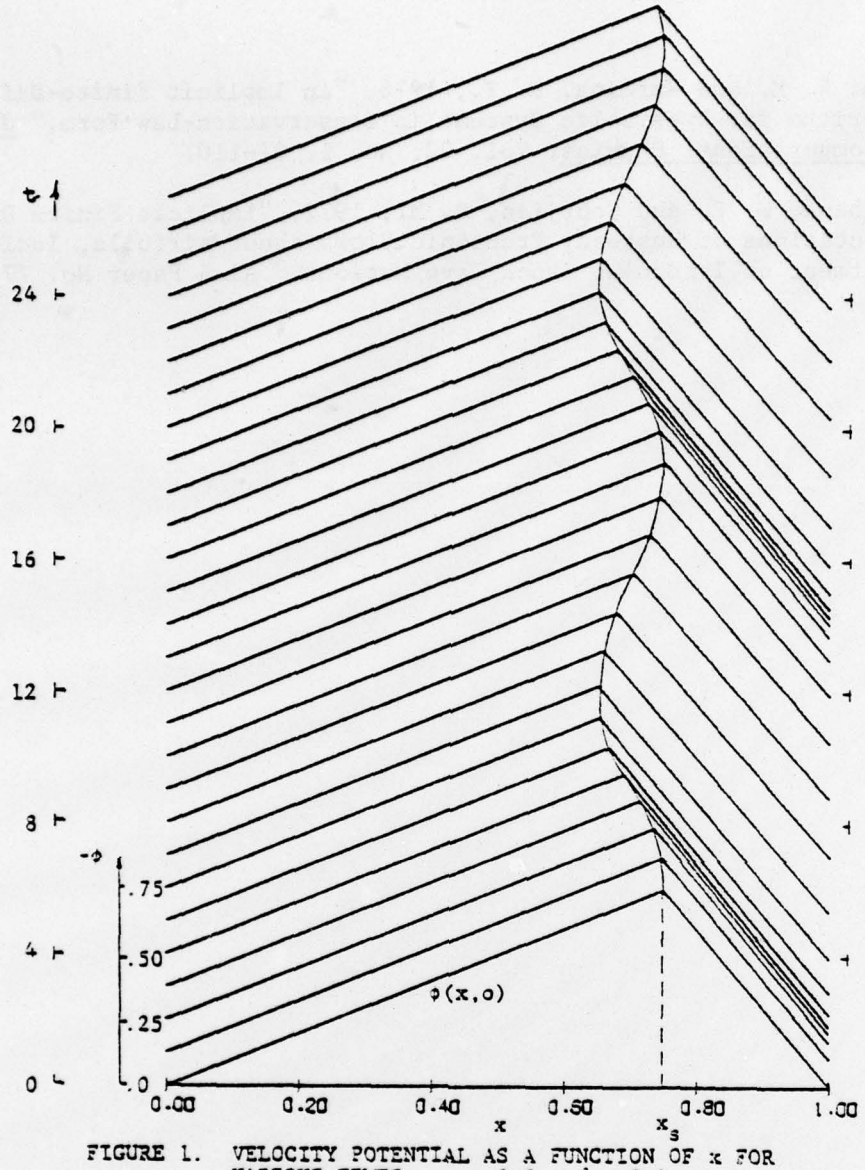

FIGURE 1. VELOCITY POTENTIAL AS A FUNCTION OF x FOR VARIOUS TIMES: $\omega = 0.5$, $\delta = 0.1$.

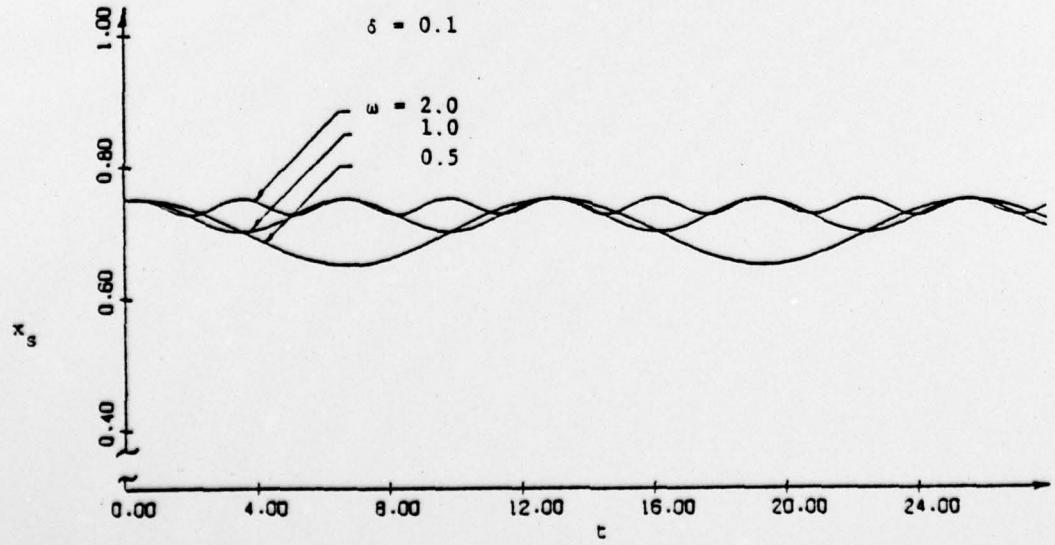

FIGURE 2. SHOCK MOTION AS A FUNCTION OF TIME FOR VARIOUS FREQUENCIES. ON THIS TIME SCALE, AND WITH $\delta = 0.1$, THE SECULAR DRIFT $O(\delta^2 t)$ IS NOT NOTICEABLE.

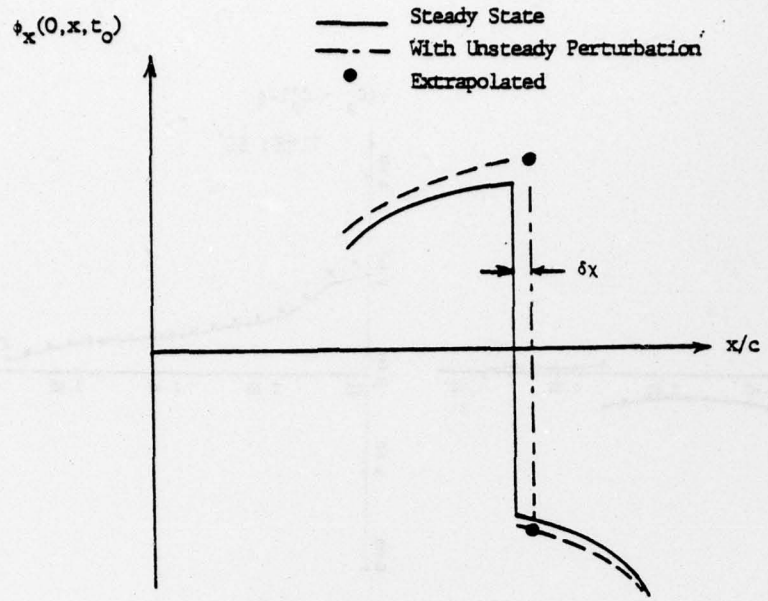

FIGURE 3. SKETCH OF STEADY STATE ϕ_x, EFFECT OF PERTURBATION $\delta\psi_x$, AND RESULTING SHOCK EXCURSION.

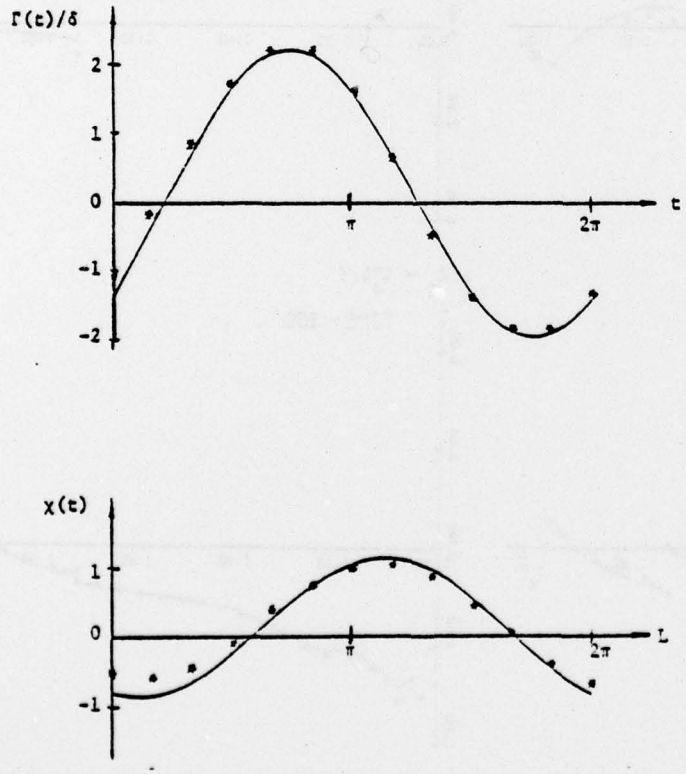

FIGURE 4. NONLINEAR (***) AND TIME-LINEARIZED(——) CIRCULATION AND SHOCK POSITION FOR THE PITCHING MOTION OF AN NACA 64A006 AIRFOIL. RESULTS SHOWN ARE FOR THE FIFTH CYCLE. THE NONLINEAR RESULTS ARE FOR $\delta = 0.1°$ AND ARE NOT YET PERIODIC. $M_\infty = 0.880$, $K = 0.48$.

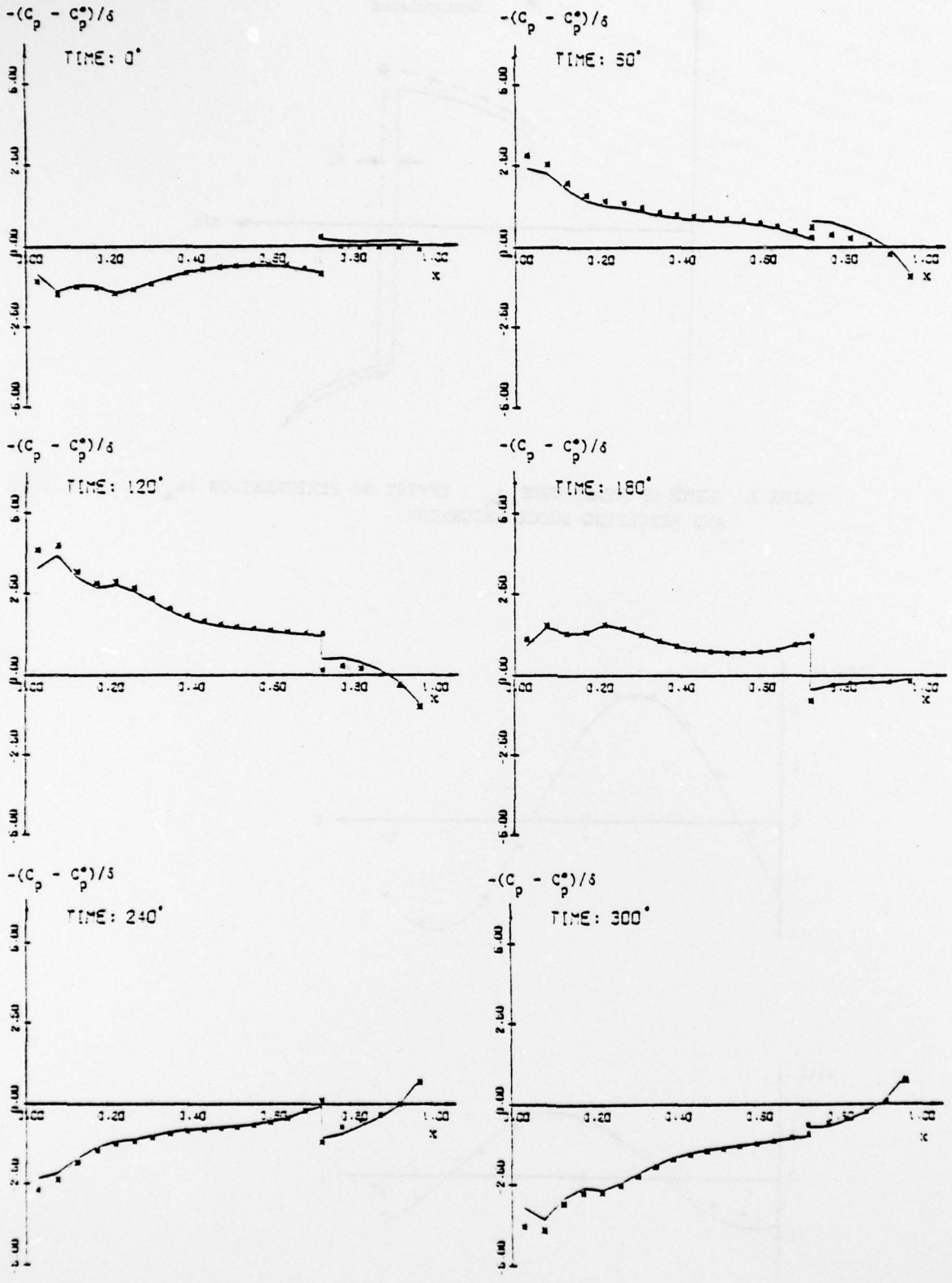

FIGURE 5. NORMALIZED NONLINEAR (****) AND TIME-LINEARIZED (——) PRESSURE PERTURBATIONS ON THE UPPER SURFACE OF AN NACA 64A006 AT SIX TIMES. PITCHING MOTION WITH M_∞ = 0.880, K = 0.48. FOR THE NONLINEAR CALCULATIONS δ = 0.1°.

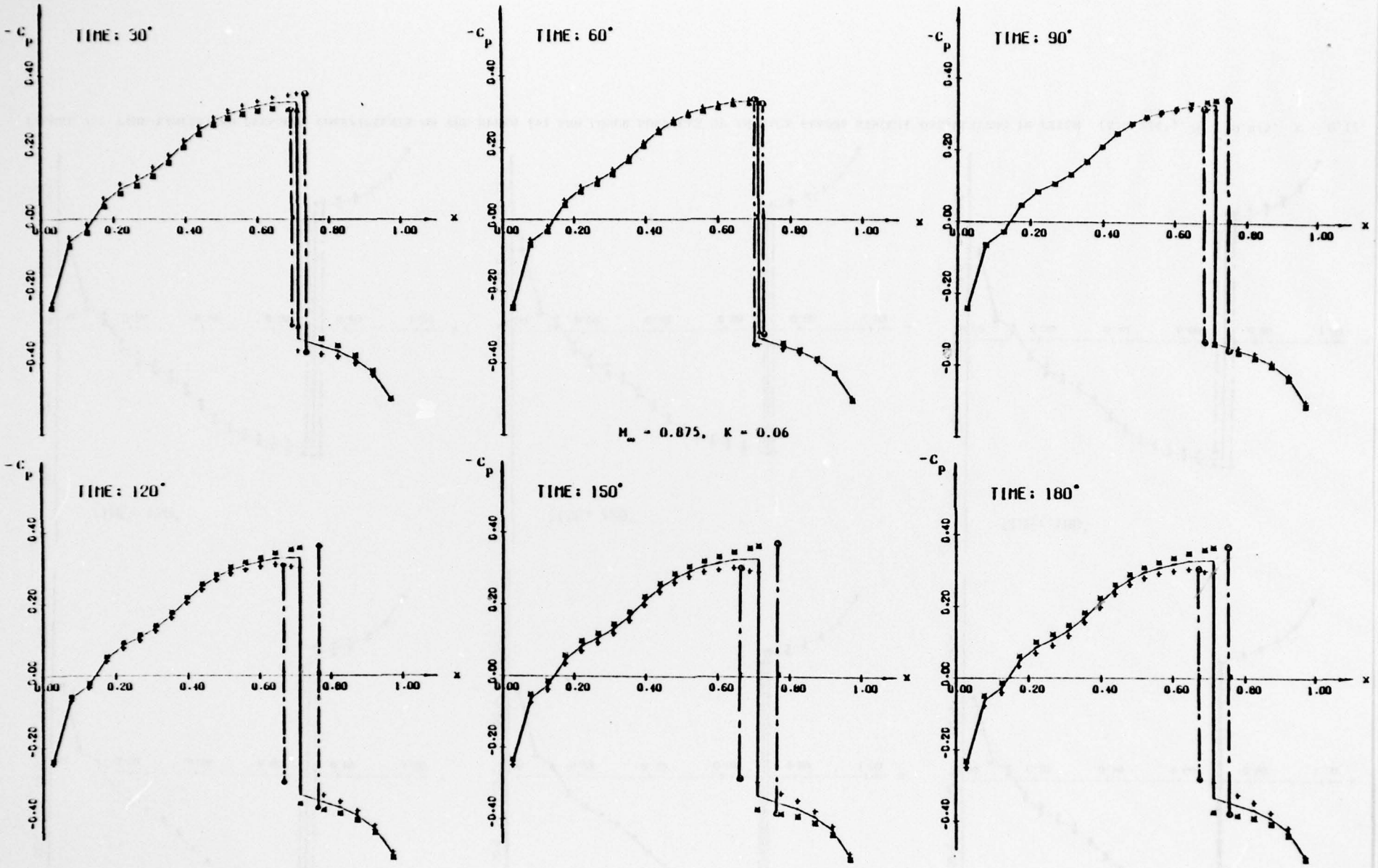

FIGURE 6. TIME-LINEARIZED PRESSURE COEFFICIENTS ON THE UPPER (+) AND LOWER (*) SURFACES OF AN NACA 64A006 AIRFOIL WITH OSCILLATING QUARTER-CHORD FLAP ($\delta = 1/4°$).

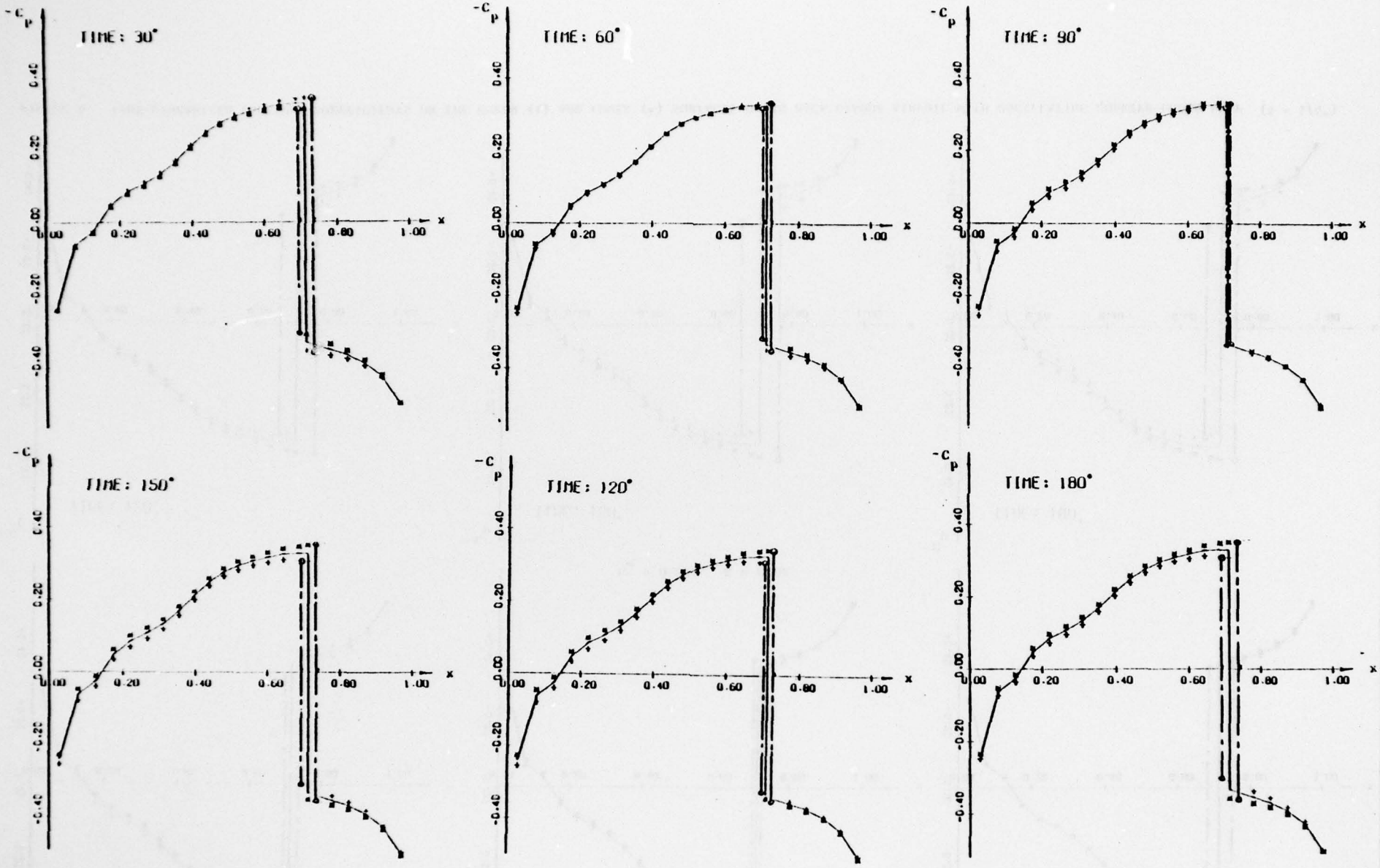

FIGURE 7. TIME-LINEARIZED PRESSURE COEFFICIENTS ON THE UPPER (+) AND LOWER SURFACES OF AN NACA 64A006 AIRFOIL OSCILLATING IN PITCH (δ = 1/4°). M_∞ = 0.875, K = 0.12.

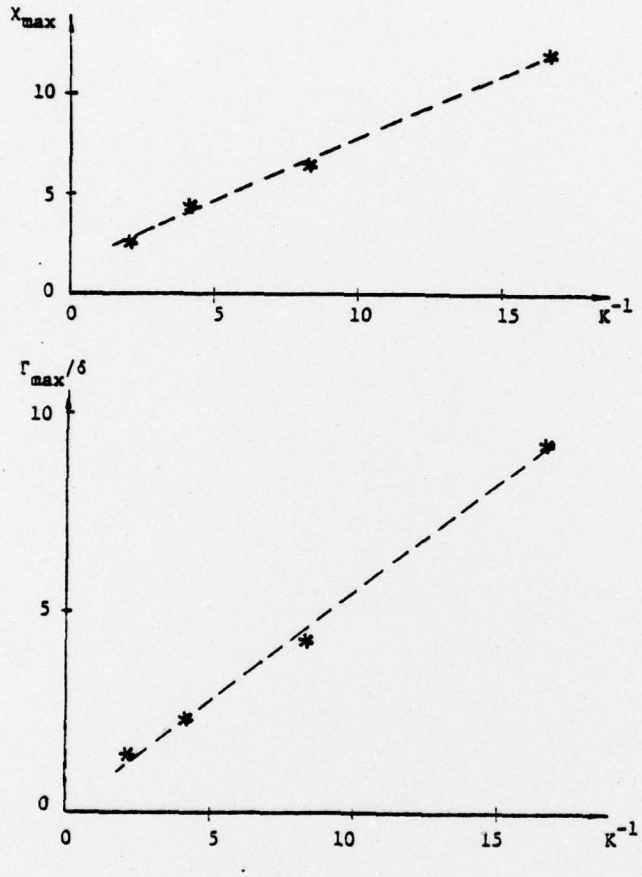

FIGURE 8. NORMALIZED MAXIMUM SHOCK EXCURSION AND CIRCULATION AS A FUNCTION OF INVERSE REDUCED FREQUENCY FOR AN NACA 64A006 AIRFOIL WITH OSCILLATING QUARTER-CHORD FLAP. $M_\infty = 0.875$.